AD-A093 067 WEAPONS SYSTEMS RESEARCH LAB ADELAIDE (AUSTRALIA) F/G 17/2
FREQUENCY WAVENUMBER BEAMFORMING BY USE OF THE TWO DIMENSIONAL --ETC(U)
JUL 80 D A GRAY
UNCLASSIFIED WSRL-0162-TR NL

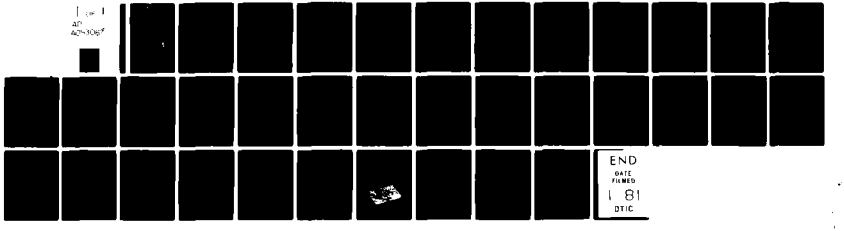

WSRL-0162-TR

AR-002-006

DEPARTMENT OF DEFENCE

DEFENCE SCIENCE AND TECHNOLOGY ORGANISATION

WEAPONS SYSTEMS RESEARCH LABORATORY

DEFENCE RESEARCH CENTRE SALISBURY
SOUTH AUSTRALIA

TECHNICAL REPORT

WSRL-0162-TR

FREQUENCY WAVENUMBER BEAMFORMING BY USE OF THE TWO DIMENSIONAL FOURIER TRANSFORM

D.A. GRAY

Approved for Public Release

JULY 1980

UNCLASSIFIED

AR-002-006

DEPARTMENT OF DEFENCE

DEFENCE SCIENCE AND TECHNOLOGY ORGANISATION

WEAPONS SYSTEMS RESEARCH LABORATORY

TECHNICAL REPORT

WSRL-0162-TR

FREQUENCY WAVENUMBER BEAMFORMING BY USE OF THE TWO DIMENSIONAL FOURIER TRANSFORM

D.A. Gray

SUMMARY

The concept of frequency wavenumber beamforming of a linear array of equispaced receivers is reviewed. The frequency wavenumber spectrum can be evaluated by using a two-dimensional Fast Fourier Transform and the properties of the resulting estimate of the frequency wavenumber spectrum are described. Particular attention is given to the distortion of the spectral power estimates due to leakage of negative frequency components.

POSTAL ADDRESS: Chief Superintendent, Weapons Systems Research Laboratory, Box 2151, GPO, Adelaide, South Australia. 5000.

DOCUMENT CONTROL DATA SHEET

Security classification of this page: UNCLASSIFIED

1 DOCUMENT NUMBERS	
AR Number:	AR-002-006
Report Number:	WSRL-0162-TR
Other Numbers:	

2 SECURITY CLASSIFICATION	
a. Complete Document:	Unclassified
b. Title in Isolation:	Unclassified
c. Summary in Isolation:	Unclassified

3 TITLE: FREQUENCY WAVENUMBER BEAMFORMING BY USE OF THE TWO DIMENSIONAL FOURIER TRANSFORM

4 PERSONAL AUTHOR(S):

D.A. Gray

5 DOCUMENT DATE: July 1980

6 6.1 TOTAL NUMBER OF PAGES: 22

6.2 NUMBER OF REFERENCES: 11

7 7.1 CORPORATE AUTHOR(S):

Weapons Systems Research Laboratory

7.2 DOCUMENT SERIES AND NUMBER

Weapons Systems Research Laboratory 0162-TR

8 REFERENCE NUMBERS

a. Task: DST 79/069

b. Sponsoring Agency:

9 COST CODE: 380 BA 326

10 IMPRINT (Publishing organisation)

Defence Research Centre Salisbury

11 COMPUTER PROGRAM(S) (Title(s) and language(s))

12 RELEASE LIMITATIONS (of the document):

Approved for public release

12.0	OVERSEAS	NO		P.R.	X	A		B		C		D		E	

Security classification of this page: UNCLASSIFIED

Security classification of this page: UNCLASSIFIED

13 ANNOUNCEMENT LIMITATIONS (of the information on these pages):

No limitation

14 DESCRIPTORS:			15 COSATI CODES:
a. EJC Thesaurus Terms	Fourier transformation Spectrum analysis Arrays Distortion Receivers Frequencies	Wavenumber Beamforming Leakage	1702
b. Non-Thesaurus Terms	Beamforming Frequency analysis Linear arrays Frequency		

16 LIBRARY LOCATION CODES (for libraries listed in the distribution):

17 SUMMARY OR ABSTRACT:
(if this is security classified, the announcement of this report will be similarly classified)

The concept of frequency wavenumber beamforming of a linear array of equispaced receivers is reviewed. The frequency wavenumber spectrum can be evaluated by using a two-dimensional Fast Fourier Transform and the properties of the resulting estimate of the frequency wavenumber spectrum are described. Particular attention is given to the distortion of the spectral power estimates due to leakage of negative frequency components.

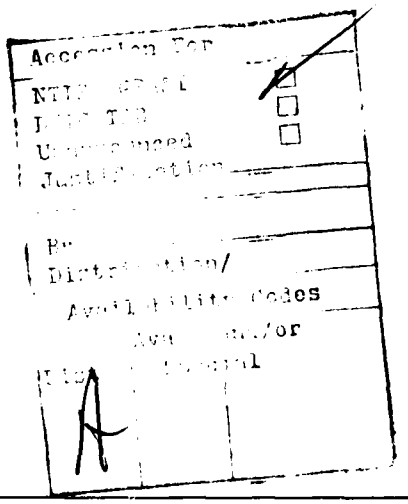

Security classification of this page: UNCLASSIFIED

TABLE OF CONTENTS

LIST OF APPENDICES

1. INTRODUCTION

Beamforming may be described loosely as the coherent processing of an array of receivers in order to ascertain the arrival directions of the incident signals or to increase the signal-to-noise ratio of a signal from a given direction. In time domain beamforming this is achieved by time delaying the receiver outputs, so that they are brought into phase coherence for a plane wave arriving from a given direction, and subsequently summing them. If the receiver outputs are first narrowband filtered then this time delay may be effected by a phase multiplication. This process is termed frequency domain beamforming.

However the choice of phase factors in frequency domain beamforming need not be restricted to those corresponding to real angles of arrival. As discussed by Booker and Clemmow(ref.1,2,3) the variable wavevector is often used instead of angular coordinates. Thus the total power incident on an array may be estimated as a function of frequency, f, and the wavevector components k_x, k_y and k_z (see references 4 and 5). It should be noted that only three of the above four variables are independant. This power estimate is termed the frequency wavenumber power spectrum (although to be pedantic it should be termed the frequency wavevector power spectrum).

For a linear array only a two dimensional formulation need be used. Thus the power spectrum is estimated as a function of the variables f, k_x and k_y. Only the independent variables f and k_x ($\equiv \frac{\sin\theta}{\lambda}$) need be used. In this paper the liberty of referring to k_x as wavenumber rather than 'the component of the wavevector along the axis of array' is taken although it should be borne in mind that wavenumber is strictly defined* as $\frac{1}{\lambda}$.

From figure 1 k may be interpreted as a spatial frequency and for a linear array of equispaced receivers the decomposition into an angular spectrum of plane wave components is mathematically equivalent to the Fourier analysis of a sampled time series into a spectrum of single frequency components.

All phase delays correspond to particular values of wavenumber which then must be interpreted in terms of the physical quantities of interest, viz., angle, frequency, and velocity of propagation. If these phase delays are effected at a number of frequencies then the resulting power spectrum is termed the frequency wavenumber power spectrum.

For a linear array of equispaced receivers it is shown in Section 2 how the frequency wavenumber spectrum can be written as a two-dimensional Fourier transform of the matrix of receiver outputs. For appropriate choices of the number of receivers and data points the Fourier transforms may be effected by use of the Fast Fourier Transform algorithm. The properties of the frequency wavenumber spectrum are discussed in Section 3 with particular attention being paid to their interpretation in terms of beamforming.

In conventional time series analysis, sidelobes from negative frequency components may distort low frequency components in the estimate of the power spectrum (see references 6 and 7). In a similar way the negative frequencies introduced by the restriction to real time series may distort other low frequency components in the estimate of the frequency wavenumber spectrum. Some measures of the sidelobe level and the power distortion due to this leakage are derived in

---

Footnote: Alternative derivations use a 2π factor.

Section 4. Finally, in Section 5 some miscellaneous remarks on the treatment of statistical data, the derivation of the spatial autocorrelation function and methods of displaying the frequency wavenumber spectrum are made.

2. THE FREQUENCY WAVENUMBER TRANSFORM

2.1 Beamforming fundamentals

In time domain beamforming the constructive interference of signals is effected by delaying the outputs of given receivers so as to bring into phase coherence any signals arriving from a given direction. For the line array of N equispaced receivers as illustrated in figure 1 the output $A(\theta, t)$ of a beam 'steered' in direction θ is given by

$$A(\theta,t) = \sum_{j=0}^{N-1} x_j\ (t - j\Delta\tau)$$

where $\Delta\tau = \frac{d\sin\theta}{c}$, d is the separation of adjacent receivers and c is the propagation velocity of the signal in the medium.

In order to determine the frequency content of a signal incident from direction θ it is necessary to Fourier analyse $A(\theta, t)$. For a continuous signal $X(\theta, f)$ an estimate of the complex amplitude of a signal of frequency f arriving from a direction θ, is given by

$$X(\theta,f) = \lim_{T\to\infty} \frac{1}{2T} \int_{-T}^{T} A(\theta,t)\exp(-2\pi ift)\ dt \qquad (1)$$

$$= \lim_{T\to\infty} \frac{1}{2T} \int_{-T}^{T} \sum_{j=0}^{N-1} x_j\ (t - j\Delta\tau)\exp(-2\pi ift)\ dt.$$

The power at this frequency and direction $S(\theta,f)$ is then given by

$$S(\theta,f) = A(\theta, f)\ A^*(\theta,f)$$

Similarly the total power incident from direction θ is given by

$$P(\theta) = \lim_{T\to\infty} \frac{1}{2T} \int_{-T}^{T} A(\theta,t)\ A^*(\theta,t)dt$$

2.2 Frequency domain beamforming

It is well known that for a narrow-band signal a time delay can be effected as a phase multiplication. By interchanging the summation and integral in equation (1) this principle may be applied to the time delays required for beamforming. It then follows that

$$X(\theta,f) = \lim_{T\to\infty} \frac{1}{2T} \int_{-T}^{T} \sum_{j=0}^{N-1} x_j(t-j\Delta\tau)\exp(-2\pi i f t)\, dt$$

$$= \sum_{j=0}^{N-1} \left(\lim_{T\to\infty} \frac{1}{2T} \int_{-T}^{T} x_j(t)\exp(-2\pi i f t)\, dt\right) \exp(-2\pi i f j\Delta\tau) \qquad (2)$$

$$= \sum_{j=0}^{N-1} X_j(f)\exp(-2\pi i f j\Delta\tau)$$

If k*, the wave-number, is defined by

$$k = f\frac{\sin\theta}{c} = \frac{\sin\theta}{\lambda} \qquad (3)$$

then

$$X(k,f) = \sum_{j=0}^{N-1} X_j(f)\exp(-2\pi i j k d) \qquad (4)$$

which is just a Fourier series of the $X_j(f)$'s. The new variable, the wave-number, has a direct physical significance in that it is (apart from a factor c) the spatial frequency of the incident plane wave in the direction of the array axis. This is diagrammatically illustrated in figure 1. This interpretation of wavenumber as a spatial frequency allows a very useful analogy between time series analysis and frequency domain beamforming. The spatial series $X_j(f), j = 0,1...N-1$ may be considered as equivalent to a time series of N data points and the resolution into spatial frequencies or wave-number expressed in equation (4) of this spatial series is equivalent to the resolution of a time series into its frequency components. This idea was first put forward by Booker and Clemmow(ref.1).

FOOTNOTE: As discussed in the introduction, wavenumber is the magnitude of a vector, the wavevector, the direction of which is orthogonal to the wavefront. However, since only one dimension is considered here wavenumber is defined in terms of the projection along the array axis. Alternative definitions involve a 2π factor.

2.3 Application to discrete finite time series

The derivation of frequency domain beamforming in the preceeding section assumed that output of each receiver was a continuous time series running from $t = -\infty$ to $t = +\infty$. In practice the time series is only observed over a finite interval and often only sampled data is available. Under these conditions the phase delays effect not a true but a cyclic time delay; this is demonstrated in Appendix I. As discussed in Appendix I and references 8 and 9 the error associated with this approximation to the true time delays can be minimized by choosing M (the number of data points) to satisfy

$$M \gg \frac{Nd}{c\tau_o} .$$

For discrete sampled data the continuously variable vector $x_j(t)$ is replaced by the matrix $X \equiv x_j(\ell\tau_o)$ abbreviated to $x_{j\ell}$ where j, as before, runs over the receivers 0,1,...,N-1 and ℓ representing the time samples will in general take the values 0,1,...,M-1 and τ_o is the sampling interval. The corresponding expression from X(k,f) now becomes

$$X(k,f) = \sum_{j=0}^{N-1} \sum_{\ell=0}^{M-1} x_{j\ell} \exp(-2\pi ikjd) \exp(-2\pi if\ell\tau_o) . \qquad (5)$$

While X(k,f) is still a continuous function of k and f it follows, since the transform is discrete that not all values of X(k,f) are independent. The maximum number of independent values can be generated by finding a complete set of orthogonal vectors. The most convenient set of vectors to choose are the $\frac{M}{2}$ sine and cosine waves whose periods are integer subdivisions of the observation interval and the N complex spatial frequencies whose spatial periods are integer subdivisions of the array aperture. Once these orthogonal set of vectors have been determined the value of X(k,f) for an arbitrary k and f can be expressed as a linear combination of these orthogonal ones. The fundamentals, Δf and Δk of these orthogonal sets of frequencies and wavenumbers are given by

$$\Delta f\tau_o = \frac{1}{M}$$

and

$$\Delta kd = \frac{1}{N} .$$

Multiples of Δf and Δk are termed the frequency and wavenumber bins respectively. The set of MN orthogonal (in a two-dimensional sense) vectors are

$$\exp(-2\pi i\mu j/N) \exp(-2\pi i\nu\ell/M)$$

for

$$\mu = 1,2,...,N$$

and

$$\nu = 1,2,\ldots,M .$$

Denoting $X(\mu\Delta k, \nu\Delta f)$ as $X_{\mu\nu}$, equation (4) reduces to

$$X_{\mu\nu} = \sum_{j=0}^{N-1} \sum_{k=0}^{M-1} x_{jk} \exp(-2\pi i \mu j/N) \exp(-2\pi i \nu \ell/M) \qquad (7)$$

This can now be readily recognised as a two-dimensional discrete Fourier transform. The power spectral density $S_{\mu\nu}$ is given by

$$S_{\mu\nu} = X_{\mu\nu} X^*_{\mu\nu}$$

and $S_{\mu\nu}\ \Delta f\ \Delta k$ represents the power incident on the array within a frequency range of $(\nu \pm \frac{1}{2})\ \Delta f$ and a wavenumber range of $(\mu \pm \frac{1}{2})\ \Delta k$.

By choosing M and N to be highly composite (eg powers of two), the above transformation may be effected by use of the Fast Fourier Transform algorithm and so the number of operations is reduced from the order of N^2M^2 to $NM \log_2 M \log_2 N$.

2.4 Physical interpretation

As indicated in the previous section $S_{\mu\nu}$ is an estimate of the power density incident on the array corresponding to a frequency $\nu\Delta f$ and a wavenumber $\mu\Delta k$. Since, in general, the physical quantities of interest are frequency and bearing, then wavenumber should be reinterpreted in terms of these parameters. From equation (3) the bearing θ, corresponding to a given frequency, f, and wavenumber, k, is given by

$$\sin\theta = ck/f \qquad (8)$$

Furthermore denoting $\theta_{\mu\nu}$ as the angle corresponding to the ν -th frequency bin and the μ -th wavenumber bin then

$$\sin\theta_{\mu\nu} = \frac{c\mu\Delta k}{\nu\Delta f} = \frac{c\mu N\Delta\sigma}{\nu M d} \qquad (9)$$

There are two interesting consequences that follow immediately from the above equation.

(a) Lines of constant bearing

From equation (8) a line of constant bearing is represented by a linear relationship between k and f the gradient of which is $c/\sin\theta$ *. If f and k are plotted as the two axes of a two-dimensional plot then as indicated in figure 2 lines of constant bearing will run radially outwards from the origin with a slope proportional to $c/\sin\theta$. Since the input time series is real it follows that the negative frequency components are mirror images of the positive ones with opposite k (see later). In figure 2 the lines corresponding to the two endfire beams and the broadside beam have been shown. The frequency $f_{\frac{1}{2}}$ is that corresponding to the half-wavelength of the array.

(b) Physical region

For real values of θ, $\sin\theta$ lies between ± 1 but as can be seen from equation (3) for low values of f, $|\frac{ck}{f}|$ can be greater than unity, eg, f = 0, which would imply that $|\sin\theta| > 1$. In the remainder of this article the region in which $|\sin\theta| \leq 1$, ie, $|f| \leq c.|k|$ will be termed the "physical region" and the region where $|f| > c.|k|$, the "non-physical region". The physical region represents plane wave signals incident on the array from angles lying between $\pm 90^\circ$.

The crosshatched areas in figure 2 represents the physical region and is bounded by the lines corresponding to the two endfire directions of $\pm 90^\circ$. The number of frequency-wavenumber bins lying within the physical region can easily be related to the half-wavelength of the array. At the half-wavelength of the array

$$f_{\frac{1}{2}} = \frac{c}{2d},$$

and substituting in equation (9) this implies that

$$\sin\theta_{N/2,\rho} = \frac{c\rho}{f_{\frac{1}{2}}} Md$$

$$= \frac{2\rho}{M} \text{ for } \rho = \frac{-M}{2},\ldots,\frac{M}{2}.$$

It trivially follows that since $|\rho| \leq \frac{M}{2}$ all the wavenumber bins correspond to physical directions. For frequencies f less than $f_{\frac{1}{2}}$ it directly follows that any value of ρ such that $|\rho| < \frac{Mf}{f_{\frac{1}{2}}}$ will correspond to a real direction.

*FOOTNOTE: In the figure f and k are treated as continuous variables; for sampled data a matrix of data should be superimposed on the diagram as shown. The interdot spacings are Δk and Δf along the wavenumber and frequency axis respectively.

(c) Non-physical region

As discussed above, contributions to the power spectrum lying within the "nonphysical region" do not correspond to a real signal incident upon the array. Some possible interpretations of components in this region are:

(i) As illustrated in figure 3 and discussed in greater detail in Section 3.2, leakage from either the frequency-time transform or the wavenumber-space transform gives rise to contributions within this region. This is especially true of the negative frequency sidelobes which are discussed in greater detail in Section 4. Sidelobes of the frequency-time transformation can be differentiated from lines of constant bearing since they are parallel to the frequency axis and do not run radially outwards from k = 0 as do lines of constant bearing. (See later).

(ii) Often effects can be transmitted through the array structure at velocities differing from those in the medium. For example, at a quarter wavelength the physical region would be doubled if the velocity of propagation through the array was half that through the surrounding medium. This is particularly common in acoustic arrays, whereby vibrations of the array structure can propagate along the array and excite the hydrophone receivers.

3. APPLICATION OF THE TWO-DIMENSIONAL FAST FOURIER TRANSFORM TO BEAMFORMING

In this section some properties of the two-dimensional discrete transform will be discussed with particular emphasis being placed on the interpretation of these properties from a beamforming viewpoint.

3.1 Symmetries

Since

$$S_{\rho\nu} = \left| \sum_{j=0}^{N-1} \sum_{k=0}^{M-1} x_{jk} \exp(-2\pi i \rho j/N) \cdot \exp(-2\pi i \nu k/M) \right|^2$$

it immediately follows that

$$S_{\rho \pm pN\ \nu \pm qM} = S_{\rho\nu}$$

for p and q integers. This periodicity in frequency and wavenumber is a consequence of the discrete temporal and spatial sampling respectively. This results in a block periodic structure as indicated in figure 2. Also the x_{ij}'s are real and so as a result (see Appendix II) it follows that

$$S_{N-\rho\ M-\nu} = S_{\rho\nu}$$

and (10)

$$S_{N-\rho\nu} = S_{\rho\ M-\nu} .$$

The physical interpretation of equations(10) is that the positive frequency components from a direction ϕ and negative frequency components from $\phi + 180^\circ$ are identical for a given value of f. At a given frequency the positive and the corresponding negative wavenumber terms have no such symmetry since they correspond to opposite velocities of the projected wavenumber along the array axis.

Note that for the wavenumbers to run contiguously from angles corresponding to $\frac{-\pi}{2}$ to $\frac{\pi}{2}$ the terms in equation (10) should be rearranged to

$$S'_{N/2+\rho\nu} = S_{\rho\nu}$$

and

$$S'_{\rho\nu} = S_{N/2+\rho\nu} \text{ for } \rho = 0,1,\ldots,N/2-1 .$$

As shown in Appendix II the d.c. and Nyquist terms require special treatment.

3.2 Response to a complex sinusoid

As discussed in Section 2.3 the two-dimensional Fourier transform is a decomposition of the matrix X into orthogonal plane waves which are harmonics of $\exp(-2\pi i\Delta kx)$ and $\exp(-2\pi i\Delta ft)$. It follows that any plane wave input which is the (k,p)th harmonic of this fundamental will contribute zero to terms in $S_{\rho\nu}$ for $\rho \neq k$ and $\nu \neq p$. For plane waves which are not exact multiples of the spatial and temporal harmonics the power will be distributed among the $S_{\rho\nu}$'s and, by analogy with time series analysis, this 'leakage' may be specified by a response function. This response function $H_{\rho\nu}$ (k,f) is the $S_{\rho\nu}$ resulting from a plane wave of frequency f and a wavenumber k. The response function may be thought of as a generalization of the polar diagram of the array since it includes all frequencies and extends the response into the 'non-physical' region (see Section 2.4). It also holds that the observed output from an arbitrary signal is given by the convultion of the true frequency wavenumber spectrum of the signal with the response function.

Furthermore, since for a complex sinusoid of unit amplitude the data x_{jp} is given by the product

$$\exp(2\pi ifj\tau_o)\ \exp(2\pi ikpd)$$

it follows that $H_{\rho\nu}(f,k)$ decomposes into the product

$$W_\rho(k)\ F_\nu(f) \qquad (11)$$

where

$$F_\nu(f) = \frac{\sin^2 \pi M(f\tau_o - \frac{\nu}{M})}{M^2 \sin^2 \pi(f\tau_o - \frac{\nu}{M})}$$

and

$$W_\rho(k) = \frac{\sin^2 \pi N(kd - \frac{\rho}{N})}{N^2 \sin^2 \pi(kd - \frac{\rho}{N})} .$$

As a result of the factorization in expression (11) many of the properties of the response function may be treated separately in spatial and temperal co-ordinates.

3.2.1 Leakage

Leakage can occur from either the frequency or the wavenumber transform and the combined effect is given by equation (11).

In particular, each term in equation (11) is of the form $G(\phi) = \frac{\sin^2 P(\phi-\phi_o)}{P^2 \sin^2 (\phi-\phi_o)}$

where P is either the number of hydrophones or time samples and ϕ represents either $2\pi k$ or $2\pi f$. This function is plotted in figure 4 where $\Delta\phi$, the separation of the zeros and also the bin width, is either the reciprocal of the observation interval or the array aperture. The leakage into the various bins is determined by the value of the appropriate response function at the multiples of $\Delta\phi$. For example in figure 4 when $\phi_o(1)$ is an exact multiple of $\Delta\phi$ there is no leakage into other bins since they correspond to the zeros of $G(\phi)$. The worst possible case is when $\phi_o(2)$ lies halfway between two bins as illustrated in figure 4 and the power is equally distributed between the two adjacent bins. In each case the power is approximately 3.9 dB down on the true power. In the extreme case of both the frequency and wavenumber lying exactly between adjacent cells it follows from expression (11) that the power in the adjacent cells is reduced by 7.8 dB.

There is an interesting consequence of the multiplicative effect of equation (11) which has a simple physical interpretation. The polar diagram as a function of k is only dependent on the frequency f through a scaling factor which is just F(f). The physical interpretation of this is that frequency components which 'leak' from the time-frequency transformation are beamformed in k-space but with a reduced amplitude. The invariance of the response function W(k) on frequency is one of the advantages of using a frequency wavenumber as opposed to a frequency bearing representation.

To illustrate these considerations, two response functions for a 32 element array are plotted in figures 3 and 5. These functions are plotted as a continuous function of wavenumber but the frequencies were evaluated at multiples of the frequency bin Δf where the highest frequency corresponded to $\lambda/2$ of the array. In figure 3 the complex sinusoid was an integer multiple of Δf and no frequency leakage is apparent. However in figure 5 since the frequency was chosen to lie halfway between two adjacent bins, leakage caused significant contributions to the resulting spectrum at all frequencies. The radical difference between these two spectra show the importance of choosing a frequency resolution which is finer than that of the expected line width of data or weighting the time series to reduce leakage.

Another advantage of using the frequency wavenumber representation is shown in figure 5. If the frequency resolution is inadequate and leakage does occur then peaks of the 'leaked'frequency terms run parallel to the frequency axis. This, even with noise present, serves to distinguish them from broadband targets of a constant bearing which would run radially from the centre, (see also figure 6).

3.2.2 Ripple

Often it is required to estimate more than either the M/2 frequency bins or the N wavenumber bins. One important reason for this is that due to the fact that the spectra corresponding to sinusoids with wavenumber or frequency components lying between bins will, due to leakage, have a ripple, the depth of which can be up to 7.8 dB. This ripple may lead to false conclusions. Another reason, particularly valid for the spatial transform, is that the number of spectrum points is insufficient and it may be desirable to interpolate between them. A simple solution to either problem is to double the number of beams steered; this reduces the spatial ripple to less than 1 dB.

Fortunately a simple way of generating these redundant beams is to add a block of N (or M in the time domain) zeros to the appropriate row or column of the matrix. The required number of beams are generated by an FFT or length 2N (or 2M). If further interpolation is required then more blocks of zeros should be similarly added.

3.2.3 Spatial aliasing

It is often the case that the sampling rate is sufficiently high that the frequency transformation will produce frequencies corresponding to wavelengths shorter than the half-wavelength of the array. It is well known that the polar diagram of an array at these higher frequencies may contain extra main lobes. By analogy with time series analysis, this phenomenon is termed spatial aliasing and once again has a convenient interpretation in the wavenumber representation. As discussed in Section 3.1 the frequency-wavenumber spectrum is periodic in wavenumber and in a similar way to time series analysis aliased wavenumbers fold back into the wavenumber spectrum. However, since the positive and negative wavenumbers are not symmetric as in time series analysis the aliased peaks of positive wavenumber will be present as negative wavenumber components and vice versa. An example of this is shown in figure 6 where the frequency range of a 32 element array has been extended to $3\lambda/4$ introducing aliased positive wavenumbers for a broadband target.

Once again the frequency-wavenumber representation is an appropriate mode for this analysis. This is because lines of constant bearing are folded back as straight lines which no longer run radially out from the origin but are inclined at a characreristic angle. This is illustrated in figure 6 for a simulated broadband source.

3.2.4 Windowing and shading

As can be seen from the examples of Section 3.2.2 the sidelobes of either the frequency or wavenumber transformation may often be too high. In particular the leakage of power from a strong signal through these sidelobes may distort and even hide a weaker signal. One technique to reduce these sidelobes is to multiply each data sample by a weight which is designed to reduce the sidelobes. This is termed windowing in time series analysis and shading in array beamforming. These are a number of well known weights among which are the Hamming, Parzen and Tchebyshev which can be applied in either the temporal or spatial domain. All of these although reducing sidelobes, have the inevitable effect of increasing the width of the main peak. A more complete description of the effect of shading is given in reference 11.

A general window and shading scheme can be represented by $\omega_{\rho\nu} = \omega_\rho \omega_\nu$ where ω_ρ and ω_ν are the appropriate temporal and spatial weights respectively. The matrix $x_{\rho\nu}$ is then replaced by $\omega_{\rho\nu} x_{\rho\nu}$.

3.3 The relation of the wavenumber bins to beamwidths

As discussed in Section 3.1 there are N independent wavenumber beams and as shown in the diagrammatic representation of H(k) in figure 4 adjacent beams overlap each other at their approximate 3.9 dB points. These beams are equispaced in wavenumber for all frequencies. Since the size of the 'physical region' varies linearly with frequency the invariance of H(k) has a number of important consequences when interpreted in terms of angles and are discussed below.

3.3.1 Frequency broadening

Frequency, wavenumber and angle are related by

$$k = 2\pi \frac{f \sin \theta}{c}$$

An approximation, particularly valid for small θ is that the change in angle $\delta\theta$ resulting from a change in wavenumber δk is given by

$$\delta\theta = \delta k c / 2\pi f \, . \qquad (12)$$

If δk is taken to be the constant wavenumber bin then it follows that the corresponding angular separation $\delta\theta$, or beamwidth as it is commonly known, will increase as the frequency is decreased according to equation (12). This can be shown to be true for all θ and is an expression of the well-known fact that the angular resolution of an array decreases with decreasing frequency.

3.3.2 Angular broadening at a given frequency

At broadside $\sin\theta \approx \theta$ and so the beams are approximately equispaced in angle. However towards endfire an increment of one wavenumber bin will correspond to a large angular variation. Thus the beamwidth of the endfire beams will be broader than those at broadside. Spacing beams such that the adjacent beams overlap at their 3.9 dB points is a simple way of ensuring a complete coverage with a minimum of redundancy and the frequency-wavenumber transform provides a natural formalism for attaining this.

4. NEGATIVE FREQUENCY DISTORTION

In assessing the properties of the frequency wavenumber spectrum, frequent use was made of the response function, defined to be the spectrum corresponding to a complex sinusoidal input. However a more realistic representation of the data is as a real sinusoid.

The results of time series analysis shows that in general the effect of this restriction is slight but can be significant in the treatment of low frequencies. In particular since the real sinusoid is the sum of two equal-amplitude complex exponentials of positive and negative frequencies, leakage of the negative power peaks will distort the estimate of the positive frequencies. Since the energy 'leaked' through a particular sidelobe decreases with its distance from the main

lobe, low frequency components are more likely to be distorted than higher frequency ones. This is illustrated in figure 7. Whether the interference is constructive or destructive will depend on the phase of the sinusoid. The effect of this in conventional time series analysis has been extensively discussed in references 1 and 2. In the remainder of this section the effect of these negative frequencies on the beamforming will be discussed.

4.1 Response to a real sinusoid

Ignoring phase terms the real data matrix due to a cosinusoidal input can be written

$$x_{j\ell} = \tfrac{1}{2}(x^{+}_{j\ell} + x^{-}_{j\ell})$$

where

$$x^{+}_{j\ell} = \exp(2\pi i(f' j\tau_o - k' \ell d))$$

and

$$x^{-}_{j\ell} = x^{+*}_{j\ell}.$$

For this section it is more convenient to work with the continuous tranform Y(k,f) defined by equation (5) rather than just the independent terms of equation (7).

Substituting in equation (5) the above expression for x_{j1} it follows that

$$X(k,f) = X^{+}(k,f) + X^{-}(k,f)$$

where

$$X^{+}(k,f) = \frac{1}{MN} \sum_{j=0}^{M-1} \sum_{\ell=0}^{N-1} \exp(2\pi i(f'-f)j\tau_o) \exp(-2\pi i(k'-k)\ell d).$$

and

$$X^{-}(k,f) = \frac{1}{MN} \sum_{j=0}^{M-1} \sum_{\ell=0}^{N-1} \exp(2\pi i(f'+f)j\tau_o) \exp(-2\pi i(k'+k)\ell d).$$

Defining

$$S^{+}(k,f) = X^{+}(k,f)\, X^{+*}(k,f)$$

it can readily be shown that

$$S^{+}(k,f) = \left\{\frac{\sin\pi M(f-f')\tau_o}{M\sin\pi(f-f')\tau_o}\right\}^2 \left\{\frac{\sin\pi N(k-k')d}{N\sin\pi(k-k')d}\right\}^2.$$

Similarly $S^{-}(k,f)$ defined by $X^{-}(k,f)\ X^{-*}(k,f)$ is given by

$$S^{-}(k,f) = \left\{\frac{\sin\pi M(f+f')\tau_o}{M\sin\pi(f+f')\tau_o}\right\}^2 \left\{\frac{\sin\pi N(k+k')d}{N\sin\pi(k+k')d}\right\}^2. \qquad (13)$$

The corresponding response to $x_{j\ell}$ is given by

$$S(k,f) = (X^{+}(k,f) + X^{-}(k,f))\ (X^{+*}(k,f) + X^{-*}(k,f))$$

which ignoring the cross terms reduces to

$$S(k,f) \cong S^{+}(k,f) + S^{-}(k,f).$$

Thus the amplitude of the negative frequency leakage into the positive frequency region is approximately determined by equation (13) evaluated for $f > 0$. The peak of $S(k,f)$ as for $f > 0$ as a function of k occurs at -k. This affords a simple physical interpretation that the negative frequency components which leak into the positive frequency region are beamformed as normal sinusoids with a wavenumber of -k i.e. incident upon the array from the reflected angle about broadside.

To qualitatively illustrate these features both $S^{+}(k,f)$ and $S(k,f)$ are plotted in figures 5 and 8 respectively for an array of 32 receivers and 16 independent frequencies varying from 0 to $\lambda/2$ of the array. Both of these functions have only been evaluated for the discrete values of f corresponding to centre cell when using a 32 point frequency transform.

4.2 *Negative frequency artefacts*

The height of these negative frequency sidelobes which leak into the positive frequency region (termed artefacts) will depend not only on N and M (the number of data points and receivers) but also on the frequency f' and wavenumber k' of the incident sine wave. The envelope of the negative frequency beams is given by

$$\frac{1}{4(MN)^2} \qquad \frac{1}{\sin^2\pi(f+f')\tau_o} \qquad \frac{1}{\sin^2\pi(k+k')d}. \qquad (14)$$

A useful measure, C, of this leakage is given by the ratio of the maximum value of the envelope for $f \geq 0$ to the peak of $S^{+}(k,f)$ ie

$$C = 10\ \log\left(\frac{\{S^{-}(k,f)\}\ \max\ f \geq 0}{\{S^{+}(k,f)\}\ \max}\right)$$

In most cases the approximation $\sin\pi(f + f')\tau_o \cong \pi(f + f')\tau_o$ holds and hence the maximum of expression (14) occurs for f = 0 and k = -k'. Thus C can be shown to reduce to

$$C = -20 \log M\pi f'\tau_o .$$

However

$$M\tau_o = T$$

where T is the observation interval and so f'T is just the number of periods within the observation interval. Thus

$$C = -20 \log \pi N_T$$

where N_T is the number of periods of the sine wave within the observation interval.

The extension of the above argument to the case of the discrete transform where only independent values of the two-dimensional transform are evaluated can easily be effected by means of the sampling theorem. For an input sinusoid whose frequency is centrecell then no artefacts will occur since all other frequencies occur at zeros of the response function. The worst case occurs when the frequency of the sinusoid lies exactly halfway between bins and expression C (with an extra 3.9 dB subtracted to allow for the equipartitioning of $S^+(k,f)$ into adjacent cells) describes the heights of the negative frequency artefacts.

4.3 Power distortion

When the 'leaked' negative frequencies artefacts are beamformed the resulting sidelobes will interfere with the main positive frequency lobe and as a result will distort an estimate of the power. A measure, P, of the distortion in the peak power estimate of a real sinusoid can be defined to be the ratio of $S^-(k,f)$ to $S^+(k,f)$ when both evaluated at k = k' and f = f'.

Thus

$$P = 10 \log \left\{ \frac{S^-(k',f')}{S^+(k',f')} \right\}$$

$$= 20 \log \left| \frac{\sin 2\pi M f'\tau_o}{M \sin 2\pi f'\tau_o} \right| \left| \frac{\sin 2\pi N k'd}{N \sin 2\pi k'd} \right| .$$

This varies from zero when both f' and k' are centre cell to a maximum when both are exactly between cells. In the latter case, P is given by

$$P = -20 \log \left| M \sin 2\pi f'\tau_o \right| \left| N \sin 2\pi k'd \right|$$

which can be approximated by

$$P = -20 \log 4\pi^2 M_\lambda N_T$$

where N_T is the number of periods of the sine wave in the observation interval and M_λ is the number of wavelengths projected onto the array aperture. (This latter quantity obviously varies with incident angle). Thus

$$P = C_\lambda C_T .$$

From this equation it can be seen that the distortion will be greatest at low frequencies and angles around broadside.

5. MISCELLANEOUS COMMENTS

5.1 Statistical data

In the preceding chapters the properties of the frequency wavenumber spectrum have been discussed with respect to deterministic signals. In order to treat random data, some sort of averaging is necessary to reduce the variance of the power estimates which are now random variables. Two methods for effecting this are possible.

(a) In time series analysis the ratio of the variance to the mean of the power spectral estimate is reduced by segmenting the time series into a number of blocks, estimating the power spectrum for each block and then averaging the power spectra. In a similar way the time series from each receiver are segmented into blocks of M data points and the frequency wavenumber spectrum is estimated for each block. The resulting blocks are averaged and the averaged power spectral estimates will have X^2 distribution, the ratio of the variance to the mean of these power estimates will be reduced by a factor of $\sqrt{P}$ where P is the number of averages. Since the array aperture is limited in space the segmenting into blocks is effected in the time domain.

An attractive feature of frequency wavenumber analysis is that if only independent frequency and wavenumber bins are used then detection statistics may readily be evaluated.

(b) Multiplying the data matrix x_{jl} by a window w_{jl} can easily be shown to be equivalent to convolving the Fourier spectrum of the X_{jl}'s with the Fourier spectrum of the W_{jl}'s. Since the two-dimensional convolution is essentially a weighted averaging of the $S_{\rho\nu}$'s over adjacent bins it follows that the variance of this convolved spectral estimate will be reduced. However, the bias (or lack of resolution) will be correspondingly increased.

5.2 Spatial autocorrelation function

In Section 2 it was shown that the wavenumber amplitude spectrum X(k,f) is the Fourier transform of the narrowband aperture distribution of signal $X_j(f)$. It follows directly that $S(k,f) = X(k,f)\ X^*(k,f)$ is the Fourier transform of the function

$$\frac{1}{N} \sum_{j=0}^{N-\rho-1} X_j^*(f)\, X_{j+\rho}(f) \,. \qquad (15)$$

This is easily seen to be the discrete autocorrelation function $r_\rho(f)$ of the $X_j(f)$'s. It follows that the frequency wavenumber spectrum could be alternatively derived as the Fourier transform of the narrowband spatial autocorrelation function at each frequency of interest. If an assumption of spatial stationarity is made, an alternative definition of $r_\rho(f)$ would be

$$r_\rho(f) = \langle X_j^*(f)\, X_{j+\rho}(f) \rangle \qquad (16)$$

where $\langle\rangle$ denotes the ensemble average.

Apart from the Bartlett window in equation (15) in the ensemble limit the estimators given by (15) and (16) are equivalent. In practice however the ensemble average will usually be replaced by a time average over a finite time interval and so expressions (15) and (16) will no longer be equivalent. This has an effect on a number of non-linear techniques for estimating the frequency wavenumber spectrum which are based on the use of the spatial autocorrelation function (15) or the cross power spectral matrix.

5.3 Displays

5.3.1 Choice of axes

A common alternative to frequency wavenumber analysis is to only form beams corresponding to the physical region and to form these beams at equal angular or $\sin\theta$ intervals. A lengthy comparison of the different displays is given in reference 10 where the frequency wavenumber plots are referred to as a distortionless Bearing Frequency display. An advantage of the frequency wavenumber display is that a broadband target will appear as a straight line whereas on a frequency bearing display it appears as a funnel shape. For detection purposes the eyeball matched filtering required is considerably simplified.

To convert a frequency wavenumber spectrum into a frequency - $\sin\theta$ spectrum, a simple interpolation procedure may be used: For each frequency a number of wavenumber points are Fourier Transformed, zeros are augmented to this transform and then the inverse transform is effected. The number of wavenumber points used in the forward transform should at least cover the physical region and due to sidelobe leakage there is probably considerable advantage in taking more. The number of zeros augmented will depend on the degree of interpolation required. A computational advantage of this interpolation is that it should only need to be effected at the end of an integration period on the averaged spectrum.

5.3.2 Display technique

The method chosen to display the intensity as a function of the variables frequency and wavenumber has been to use a 'hide' routine. The perspective of this can be varied in order to display features which may have been blanked out by strong targets. Two alternative methods of displaying a function of two variables are the two-dimensional intensity modulated

displays (or LOFARgrams) or contour plots ('fraz') or equi-level contours.

5.4 Analysis of real data

To illustrate some of the features of frequency wavenumber beamforming 128 data points from each of 32 hydrophones of a linear array were processed using a two dimensional Fast Fourier Transform. Zeros were appended to the end of each spatial transform resulting in 128 wavenumber bins. The frequency wavenumber power spectrum when averaged over 300 integrations is shown in figure 9 where the 40 independent frequencies range from zero to that corresponding to the half-wavelength of the array. Features such as the radial characteristics of broadband sources, spatial aliasing of low frequency array self noise and leakage into the nonphysical region are readily discernible.

6. CONCLUSIONS

Provided care is taken to avoid the errors in approximating delays as discussed Appendix I and the leakage through negative frequency sidelobes, the two-dimensional Fast Fourier Transform has been shown to be a natural and efficient way of estimating the two-dimensional frequency wavenumber spectrum. The spacing of beams which naturally overlap at their 3.9 dB points and the fact that broadband targets appear as straight lines, are two particular advantages of using a frequency wavenumber analysis. For certain problems such as array self-noise the extension of the wavenumber representation into the non-physical region is very useful.

REFERENCES

No.	Author	Title
1	Booker, H.G. and Clemnow, P.C.	"The Concept of an Angular Spectrum of Plane Waves, and its Relation to that of Polar Diagram and Aperture Distribution". Journal IEE, Vol.97, p.III, p.11, 1950
2	Bracewell, R.N.	"The Fourier Transform and its Applications". McGraw Hill, 1955
3	Burg, J.P.	"Three-Dimensional Filtering with an Array of Seismometers". Geophysics, 29, 693, 1963
4	Capon, J.	"Maximum-Likelihood Spectral Estimation" in "Topics in Applied Physics : Nonlinear Methods of Spectral Analysis". Ed S. Haykin, Vol.34, 1979
5	McDonough, R.N.	"Application of the Maximum-Likelihood Method and the Maximum Entropy Method to Array Processing". ibid.
6	Toman, K.	"The Spectral Shifts of Truncated Sinusoids". Jnl Geophys. Res. 70, 1749, 1965
7	Jackson, P.L.	"Truncations and Phase Relationships of Sinusoids". Jnl Geophys. Res. 72, 1400, 1967
8	Rudnick, P.	"Digital Beamforming in the Frequency Domain". Jnl. Acoust. Soc. Am. 46, 1089, 1969
9	Edelblute, T.J.	"Theory of Operation of Line Array Processor and Display". NUSC Report, August 1973
10	Eby, E.S., and Fein, M.O.	"A Distortionless Bearing - Frequency Display". NUSC Report, 4127, September 1971
11	Harris, F.J.	"On the Use of Windows for Harmonic Analysis with the Discrete Fourier Transform". Proc. IEEE 66, 51, 1978

APPENDIX I

PHASE DELAYS AS A CYCLIC TIME SHIFT

Let $X_j(f)$ denote the frequency output of the j^{th} receiver; it is defined by

$$X_j(f) = \sum_{l=0}^{M-1} x_j(l\tau_o) \exp(-2\pi i f l \tau_o) \qquad (I.1)$$

where τ_o is the sampling interval.

Suppose it is required to steer a beam in a direction ϕ defined by

$$p\tau_o = \frac{d\sin\phi}{c}$$

where p is some integer. (The restriction to a steering angle such that the interelement time delay is an integral multiple of the sampling rate is not essential but simplifies the following argument).

When steering in this direction $X_j(f)$ is multiplied by a phase factor of the form

$$\exp(-2\pi i f p \tau_o)$$

However since the transform in equation (I.1) is finite the phase factor corresponds not to a true time delay but rather a cyclic time delay. Thus if the input series used in (I.1) is

$$x_o, x_1, x_2 \ldots\ldots\ldots x_{M-1}$$

where

$$x_i \text{ denotes } x_j(i\tau_o)$$

then it follows that

$$X_j(f) \exp(-2\pi i f p \tau_o)$$

corresponds to a cycled version i.e.

$$\underset{\uparrow\ p^{th} \text{ position}}{x_{M-p}\ x_{M-p+1}\ x_{M-1}\ x_o\ x_1 \ldots\ldots\ x_{M-p-1}}$$

In a time delay beamformer the corresponding series would be

$$x_{-p} \cdots\cdots x_{-1}\, x_o\, x_1 \cdots\cdots x_{M-p-1}$$

Thus since the frequency domain beamformer does not have available the values $x_{-p}, \ldots, x_{-1}$ it approximates them by $x_{M-p}, \ldots, x_{M-1}$.

The magnitude of this error depends on a number of factors; the frequency of the signal, the arrival angle and the length (Mr_o) of the data record used to effect the transform (I.1). The problem has been addressed in references 3 and 4 and to minimize the effect of the cyclic time delay it is recommended that the data accumulation period (ie Mr_o) should be much greater than the time for a signal to transverse the array. This time is longest for beams steered around endfire and so the condition can be expressed as

$$Mr_o \gg N\frac{d}{c} \quad .$$

APPENDIX II

SYMMETRY PROPERTIES OF THE TWO-DIMENSIONAL SPECTRUM

The number of independent terms in the power matrix S are derived and the correct treatment of the d.c. and Nyquist terms is given.

Symmetries

Defining the following cosine and sine transforms

$$\begin{aligned} a_{\rho\nu} &= \sum_{j,k} x_{jk} \cos \frac{2\pi\rho j}{N} \cos \frac{2\pi k\nu}{M}, \\ b_{\rho\nu} &= \sum_{j,k} x_{jk} \sin \frac{2\pi\rho j}{N} \sin \frac{2\pi k\nu}{M}, \\ c_{\rho\nu} &= \sum_{j,k} x_{jk} \cos \frac{2\pi\rho j}{N} \sin \frac{2\pi k\nu}{M}, \end{aligned} \tag{II.1}$$

and

$$d_{\rho\nu} = \sum_{j,k} x_{jk} \sin \frac{2\pi\rho j}{N} \cos \frac{2\pi k\nu}{M},$$

it follows that

$$X_{\rho\nu} = a_{\rho\nu} - b_{\rho\nu} + i(c_{\rho\nu} + d_{\rho\nu}).$$

From equations (II.1) the symmetries such as

$$a_{\rho\nu} = a_{\rho M-\nu} = a_{N-\rho\nu} = a_{N-\rho M-\nu}$$

can easily be derived, with corresponding relationships holding for the $b_{\rho\nu}$, $c_{\rho\nu}$ and $d_{\rho\nu}$. An immediate consequence of the reality of the x_{jk}'s is the relation

$$X^*_{\rho\nu} = X_{N-\rho M-\nu}$$

and consequently that

$$S_{N-\rho\ M-\nu} = S_{\rho\nu}$$

It also holds that since $S_{\rho\nu}$ is given by

$$S_{\rho\nu} = (a_{\rho\nu} - b_{\rho\nu})^2 + (c_{\rho\nu} + d_{\rho\nu})^2 \tag{II.2}$$

that

$$S_{N-\rho\nu} = S_{\rho M-\nu}$$

These symmetries combine to reduce the number of independent elements by a factor of 2.

D.C. and Nyquist terms

The d.c. and Nyquist terms (corresponding to subscripts 0, $\frac{N}{2}$ or $\frac{M}{2}$) are usually calculated as the real and imaginary parts of the X_{oo} element. To estimate the power in these components by equation (II.2) is incorrect. Assuming that the d.c. and Nyquist components are stored in the real and imaginary parts of the zero-th term the correct expressions for the powers are

$$\left.\begin{aligned} S_{o\nu} &= a^2_{o\nu} + c^2_{o\nu} \\ S_{N/2\nu} &= b^2_{o\nu} + d^2_{o\nu} \\ S_{\nu o} &= a^2_{\nu o} + d^2_{\nu o} \\ \text{and} \quad S_{\nu M/2} &= b^2_{\nu o} + c^2_{\nu o} \end{aligned}\right\} \quad \nu \neq 0$$

For $\nu = 0$ the expressions are further contracted to

$$S_{oo} = a^2_{oo}$$

and

$$S_{N/2\ M/2} = b^2_{oo}$$

As a result of this decomposition and the symmetries, the number of independent power terms in $\frac{MN}{2} + 1$.

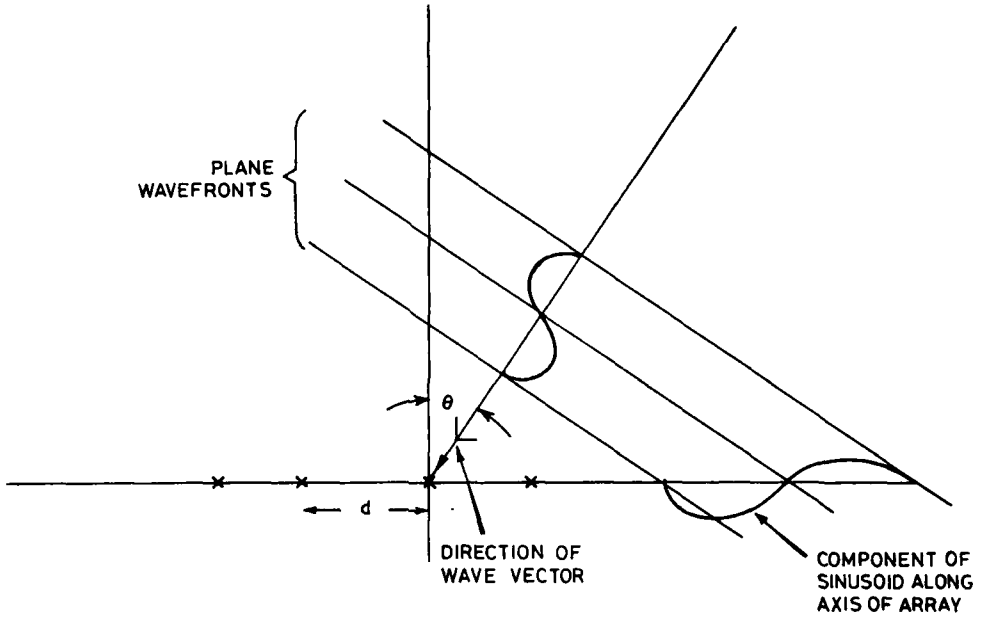

Figure 1. A linear array of equispaced receivers

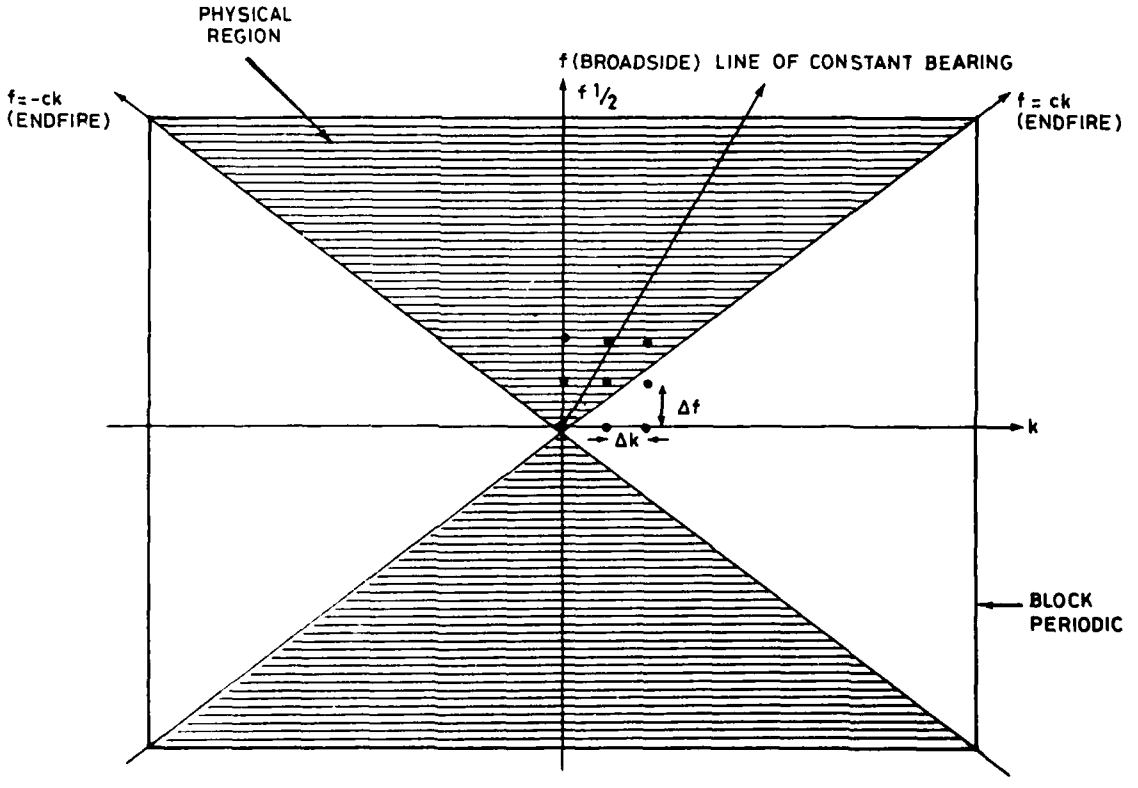

Figure 2. Frequency wavenumber plots

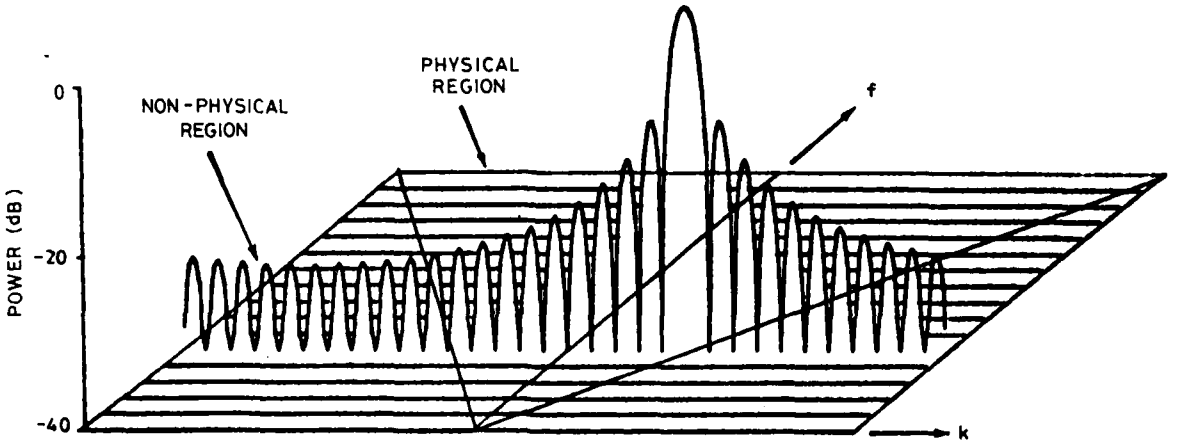

Figure 3. Side lobe leakage into non physical region

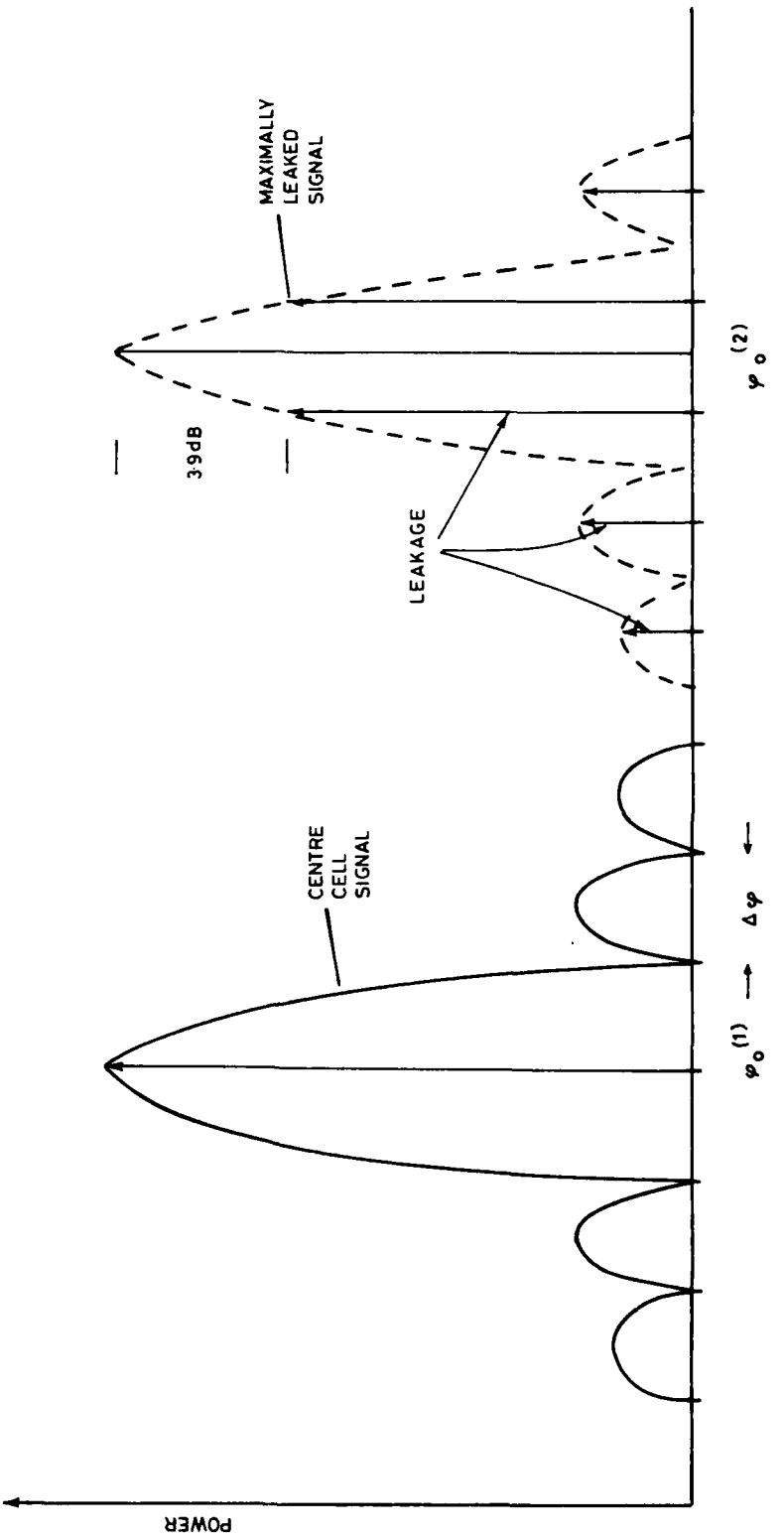

Figure 4. General response functions

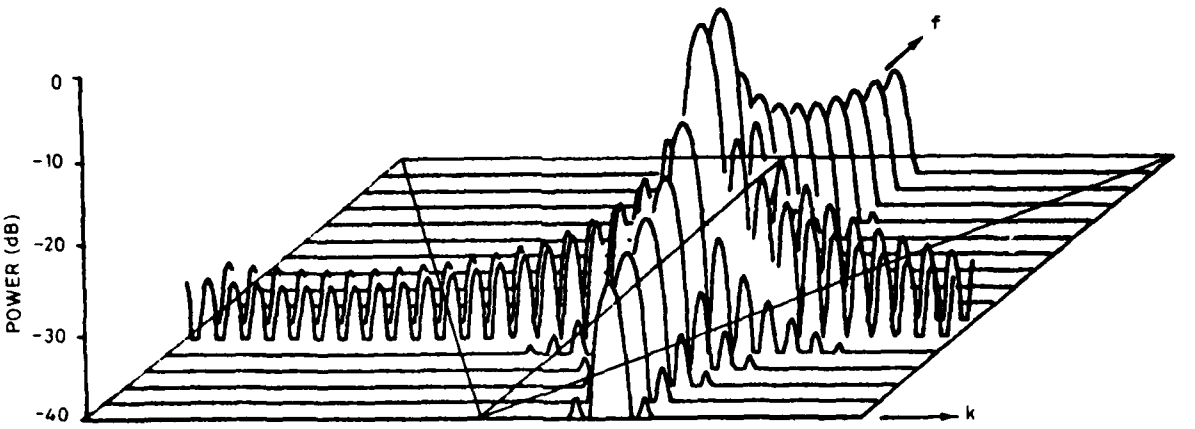

Figure 5. Response function of a maximally frequency leaked sinusoid

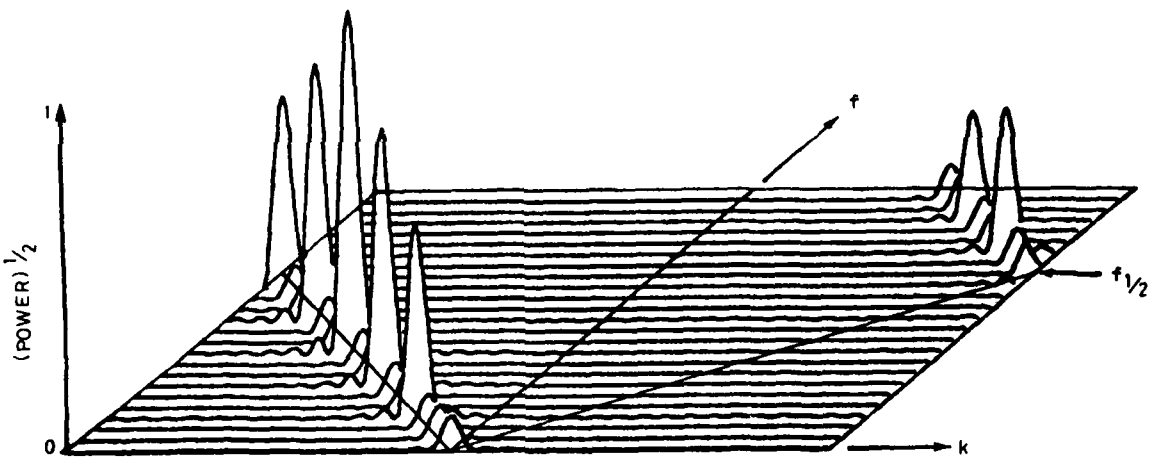

Figure 6. Spatial aliasing

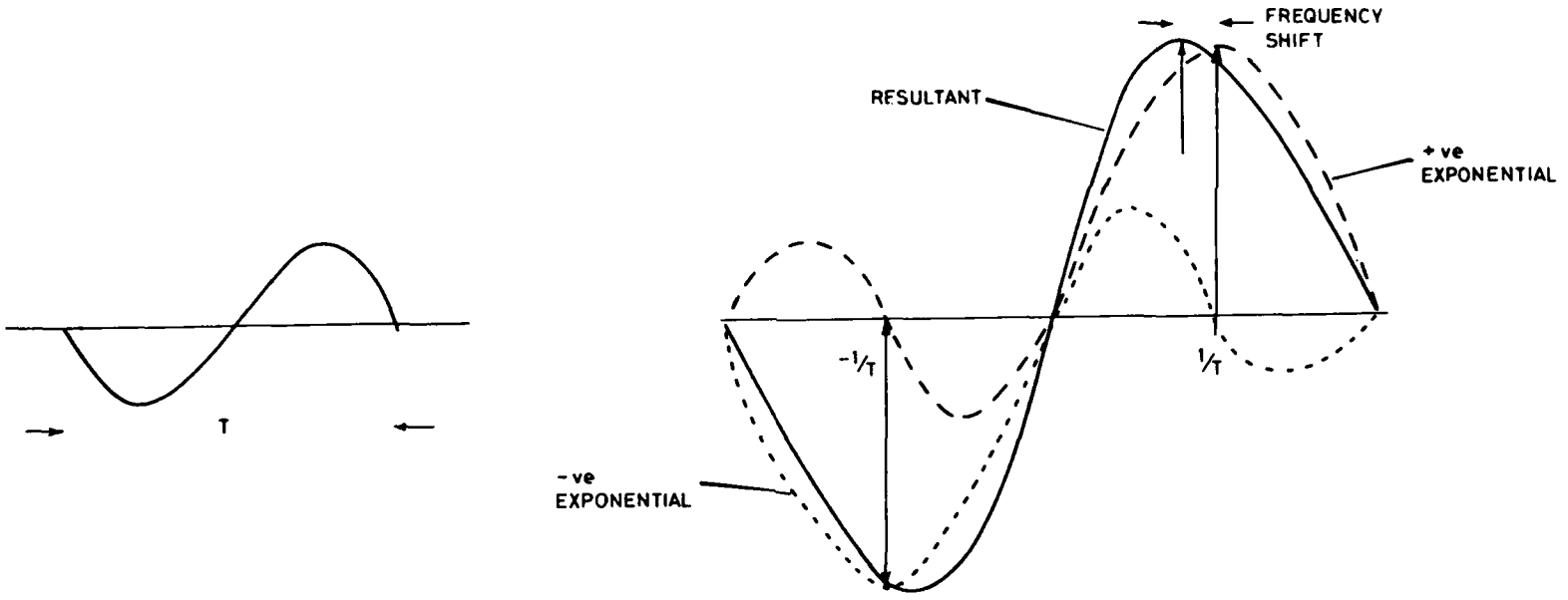

Figure 7. Coherent addition of positive and negative frequency responses

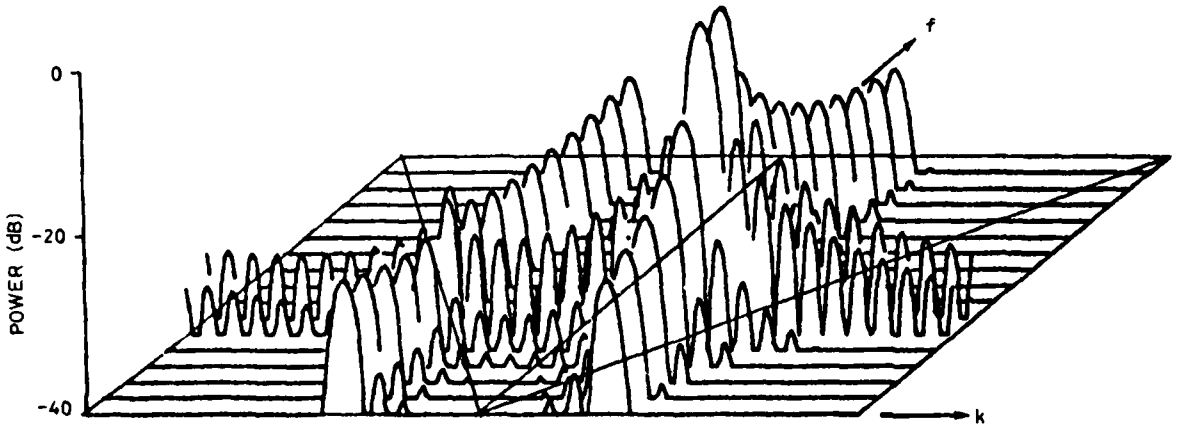

Figure 8. Response function of maximally leaked real consinusoid

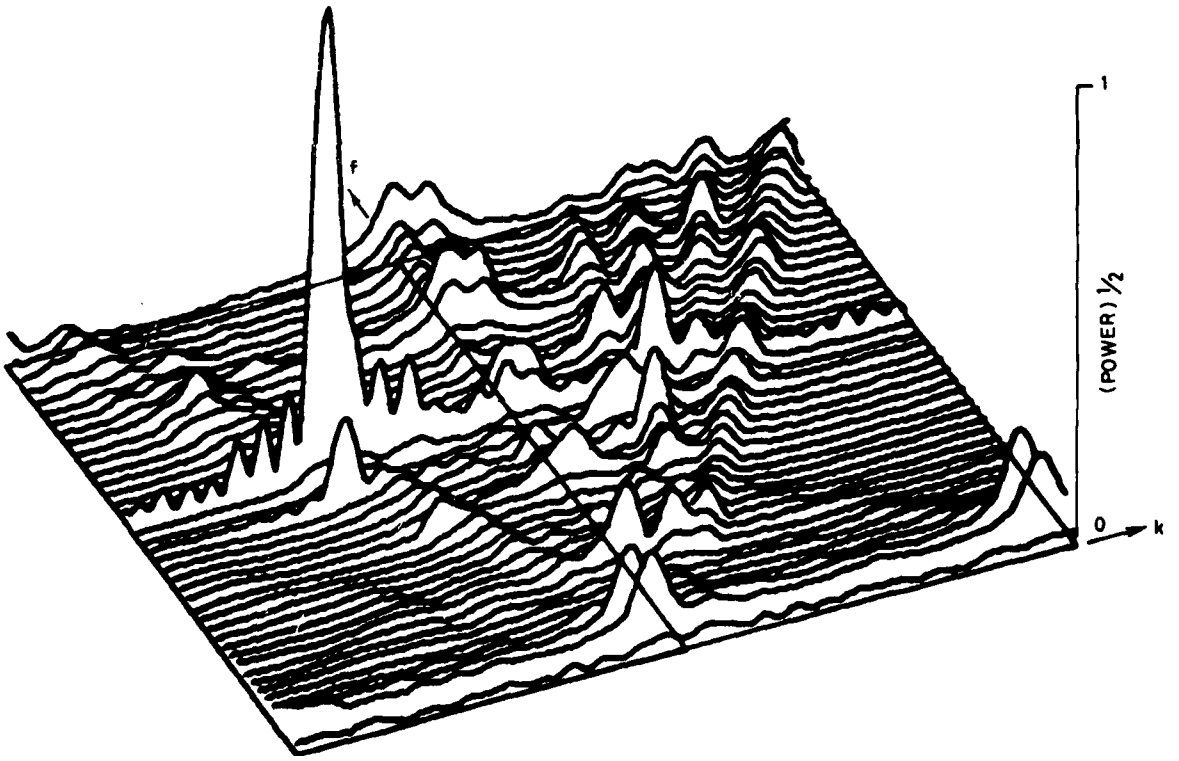

Figure 9. Frequency wavenumber spectrum for real data

DISTRIBUTION

Copy No.

EXTERNAL

In United Kingdom

Defence Scientific and Technical Representative, London	1
Dr C. Hart (RN3 Div) Royal Aircraft Establishment, Farnborough	2
Dr D. Williams, AUWE Portland, Dorset	3
British Library Lending Division, Boston Spa, Yorkshire	4

In United States of America

Counsellor, Defence Science, Washington	5
Dr V.C. Anderson, MPL Scripps Institute of Oceanography, San Diego	6
National Technical Information Services, Springfield Va 22151	7
Engineering Societies Library, New York NY 10017	8
Cambridge Scientific Abstracts, Riverdale Md 20840	9

In Australia

Chief Defence Scientist	10
Deputy Chief Defence Scientist	11
Superintendent, Science and Technology Programmes	12
Director, Joint Intelligence Organisation (DDSTI)	13
Navy Scientific Adviser	14
Superintendent, Central Studies Establishment	15
Superintendent, RAN Research Laboratory	16
Dr A.S. Burgess, HMAS Watson	17
Defence Library, Campbell Park	18
Library, Aeronautical Research Laboratories	19
Library, Materials Research Laboratories	20
Defence Information Services Branch (for microfilming)	21
Defence Information Services Branch for:	
United Kingdom, Ministry of Defence, Defence Research Information Centre (DRIC)	22
Canada, Department of National Defence, Defence Science Information Service	23
United States, Department of Defense, Defense Documentation Center	24 - 35
New, Zealand, Ministry of Defence	36
Australian National Library	37
Prof. R.G. Keats, Maths Department, University, Newcastle	38
Dr A. Cantoni, Department Electronic Engineering, University, Newcastle	39

	Copy No.
WITHIN DRCS	
Chief Superintendent, Weapons Systems Research Laboratory	40
Chief Superintendent, Electronics Research Laboratory	41
Superintendent, Electronic Warfare Division	42
Superintendent, Radar Division	43
Senior Principal Research Scientist, Radar	44
Senior Principal Research Scientist, Marine	45
Dr M. Lees, Jindalee Project Group	46
Principal Officer, Ionospheric Studies Group	47
Principal Officer, Tropospheric Studies Group	48
Dr R. Clarke, Ionospheric Studies Group	49
Principal Officer, Underwater Detection Group	50
Principal Officer, Signal Processing and Classification Group	51
Mr G.C. Mountford, Signal Processing and Classification Group	52
Dr A.L. Carpenter, Underwater and Detection Group	53
Mr A.P. Clarke, Signal Processing and Classification Group	54
Dr D. Kewley, Underwater Detection Group	55
Dr A.K. Steele, Signal Processing and Classification Group	56
Dr D.G. Cartwright, Signal Processing and Classification Group	57
Dr G. Gartrell, Signal Processing and Classification Group	58
Author	59 - 60
DRCS Library	61 - 62
Spares	63 - 68

The official documents produced by the Laboratories of the Defence Research Centre Salisbury are issued in one of five categories: Reports, Technical Reports, Technical Memoranda, Manuals and Specifications. The purpose of the latter two categories is self-evident, with the other three categories being used for the following purposes:

Reports	:	documents prepared for managerial purposes.
Technical Reports	:	records of scientific and technical work of a permanent value intended for other scientists and technologists working in the field.
Technical *Memoranda*	:	intended primarily for disseminating information within the DSTO. They are usually tentative in nature and reflect the personal views of the author.